

## ULTRAVIOLET LIGHT CURVES OF SUPERNOVAE WITH *SWIFT* UVOT

PETER J. BROWN<sup>1</sup>, STEPHEN T. HOLLAND<sup>2,3,4</sup>, STEFAN IMMLER<sup>2,4</sup>, PETER MILNE<sup>5</sup>, PETER W. A. ROMING<sup>1</sup>,  
NEIL GEHRELS<sup>2</sup>, JOHN NOUSEK<sup>1</sup>, NINO PANAGIA<sup>6,7,8</sup>, MARTIN STILL<sup>9</sup>, & DANIEL VANDEN BERK<sup>1</sup>

*Draft version October 22, 2018*

### ABSTRACT

We present ultraviolet (UV) observations of supernovae (SNe) obtained with the UltraViolet/Optical Telescope (UVOT) on board the *Swift* spacecraft. This is the largest sample of UV light curves from any single instrument and covers all major SN types and most subtypes. The UV light curves of SNe Ia are fairly homogenous while SNe Ib/c and IIP show more variety in their light curve shapes. The UV-optical colors clearly differentiate SNe Ia and IIP, particularly at early times. The color evolution of SNe IIP, however, makes their colors similar to SNe Ia at about 20 days after explosion. SNe Ib/c are shown to have varied UV-optical colors. The use of UV colors to help type SNe will be important for high redshift SNe discovered in optical observations. These data can be added to ground based optical and near infrared data to create bolometric light curves of individual objects and as checks on generic bolometric corrections used in the absence of UV data. This sample can also be compared with rest-frame UV observations of high redshift SNe observed at optical wavelengths.

*Subject headings:* cosmology: distance scale–ISM: dust, extinction– galaxies: distances and redshifts– supernovae: general–ultraviolet: general

### 1. ULTRAVIOLET SN OBSERVATIONS

From the earliest photon signal from a SN during the shock breakout, the UV light from supernovae contains many clues about the explosion and the environment, with application to both nearby and high-redshift SNe. The contribution of UV light to the bolometric luminosity can be significant, particularly at the earliest epochs when the high temperature yields a large UV flux. Because line blanketing in the UV is dominated by iron peak elements, the UV brightness is sensitive to the ionization level (cf. Dessart et al. 2007) and differences in metallicity (Nugent et al. 1997; Lentz et al. 2000). The large UV extinction observed in most extinction curves also allows UV observations to better constrain the reddening to individual objects (Jeffery et al. 1994).

The first observation of UV light from a SN was performed by the Orbiting Astronomical Observatory in 1972, revealing the UV faintness of a type I SN (Holm, Wu & Caldwell 1974). The International Ultraviolet Explorer (IUE) built up a larger sample with UV spectroscopic observations of 25 SNe

(Cappellaro, Turatto, & Fernley 1995), with excellent light curves for SNe IIL 1979C (Panagia et al. 1980) and 1980K, the Ib 1983N, Ia 1992A (Kirshner et al. 1993), as well as the II-pec 1987A (Pun et al. 1995). The spectacular event of SN 1987A was also observed in the UV by the Astron Station (Lyubimkov 1990). The Hubble Space Telescope (HST) has added excellent UV spectroscopic and photometric data for another  $\sim 30$  SNe (see Panagia 2003 for a review of IUE and HST UV observations up to that time). The Galaxy Evolution Explorer (Gal-Yam et al., in preparation), and the Optical Monitor on the XMM-Newton mission (cf. Immler et al. 2005) have added a few more observations each. Rest-frame UV observations of higher redshift SNe observed in the optical from the ground are also now being regularly obtained (Astier et al. 2006; Foley et al. 2007; Ellis et al. 2008).

The latest UV observatory is *Swift* UVOT (Romig et al. 2005). The *Swift* observatory's quick response capability and short term scheduling, necessitated by the unpredictable and variable behavior of individual gamma ray bursts (GRB), also allows newly discovered SNe to be observed quickly and with well sampled light curves (Gehrels et al. 2004). Data are available in a matter of hours, and observing times and filter combinations can be changed on a day to day basis depending on what is seen in recent observations. Thus far, *Swift* has focused on nearby SNe ( $z \lesssim 0.02$ ) for which high quality data can be obtained with only a small impact on spacecraft operations and *Swift*'s primary mission to detect and observe GRBs. SN observations are performed under *Swift*'s Target of Opportunity (ToO) program<sup>10</sup>. A dedicated website<sup>11</sup> has been set up that gives the status of *Swift* SN observations, images and regularly updated light curves for the benefit of the community.

<sup>1</sup> Pennsylvania State University, Department of Astronomy & Astrophysics, University Park, PA 16802, USA

<sup>2</sup> Astrophysics Science Division, Code 660.1, NASA/Goddard Space Flight Center, Greenbelt, MD 20770, USA

<sup>3</sup> Universities Space Research Association, 10227 Wincopin Circle, Suite 221, Columbia, MD 21044, USA

<sup>4</sup> Centre for Research and Exploration in Space Science and Technology Code 660.8, NASA/GSFC, Greenbelt, MD 20770, USA

<sup>5</sup> Steward Observatory, University of Arizona, 933 North Cherry Avenue, Tucson, AZ 85721

<sup>6</sup> Space Telescope Science Institute, 3700 San Martin Drive, Baltimore, MD 21218, USA

<sup>7</sup> INAF-Osservatorio Astrofisico di Catania, Via S. Sofia 78, I-95128 Catania, Italy

<sup>8</sup> Supernova Ltd., OYV #131, Northsound Road, Virgin Gorda, British Virgin Islands

<sup>9</sup> Mullard Space Science Laboratory, Department of Space and Climate Physics, University College London, Holmbury St Mary, Dorking, Surrey, RH5 6NT, UK

<sup>10</sup> <http://www.swift.psu.edu/too.html>

<sup>11</sup> see [http://swift.gsfc.nasa.gov/docs/swift/sne/swift\\_sn.html](http://swift.gsfc.nasa.gov/docs/swift/sne/swift_sn.html)

TABLE 1  
Swift UVOT FILTER CHARACTERISTICS

Filter	$\lambda_{central}$ (Å)	FWHM (Å)	Zeropoint (mag)
uvw2	1928	657	$17.35 \pm 0.03$
uvm2	2246	498	$16.82 \pm 0.03$
uvw1	2600	693	$17.49 \pm 0.03$
<i>u</i>	3465	785	$18.34 \pm 0.020$
<i>b</i>	4392	975	$19.11 \pm 0.016$
<i>v</i>	5468	769	$17.89 \pm 0.013$

In this paper we present some of the overall UV properties of SNe seen in our sample. In particular, we contrast the UV light curve shapes and colors of the different types, which is best done with a sample observed with the same instrumental setup. Understanding the brightness (relative to the optical) and temporal behavior should assist future observatories to understand the sampling and depth necessary to characterize a UV light curve.

## 2. OBSERVATION SUMMARY

Swift UVOT has observed 48 SNe between March 2005 (Brown et al. 2005) and August 2007. UVOT typically observes SNe with three UV and three optical broadband filters. The central wavelengths and widths are given in Table 1 (Poole et al. 2008). Brown et al. (2007b) display the transmission of these filters with respect to SNe spectra. However, like IUE, they are limited to the brightest epochs of the the nearest SNe. Here we focus on results from the photometry; spectroscopic results will be presented elsewhere (Bufano et al. in prep).

Images were obtained from the *Swift* archive, and for those whose most recent processing occurred prior to 2007, the raw images and event lists were reprocessed, primarily to utilize an improved plate scale for the uvw2 images and corrections to exposure times in the headers. Exposures were aspect corrected then coadded by epoch, usually corresponding to unique observation numbers. Due to the rapid evolution of SN 2006aj/GRB060218 during the first day the exposures in the first observation number were used individually and subsequent observations coadded as usual. We performed aperture photometry using a 3'' source aperture to improve the signal to noise and minimize galaxy contamination compared to larger apertures (cf. Li et al. 2006). A background region was chosen by eye to be similar to the galaxy background near the SN. Over or undersubtraction of the underlying galaxy leads to the magnitudes being under or overestimated when the SN fades close the the galaxy level, so here we focus on the brightest epochs and less contaminated events where the galaxy contribution is less significant. Counts within a 5'' aperture around the SN were used to compute the coincidence loss correction factor (to be consistent with the calibration), and an average point spread function (psf) for each filter was used to compute the aperture correction factor from our 3'' aperture to the 5'' for which the zeropoints are calibrated (Poole et al. 2008). The light curves of those with at least 3 UV detections well above the estimated galaxy background (26 out of the 48 SNe observed during this period) are displayed on a continuous timeline in Fig. 1, with individual light curves displayed in Figs. 2 and 3. Fig. 1 illustrates the dynamic range and frequency

of Swift SN observations. The bright limit, above which coincidence losses are hard to correct, is approximately 12th magnitude in the UV. In practice this saturation limit from a bright SN or a SN on a bright galaxy background has affected the optical light curves of some of these SNe but not the UV light curves. The faint limit can be as deep as about 21 mag but observations are typically terminated once the galaxy light dominates within the aperture.

## 3. LIGHT CURVES

The temporal behavior of the UV light varies with SN type. Fig. 2 shows UVOT lightcurves for the individual SNe Ia. SNe Ia rise to a maximum in the UV peaking just before the optical. Similar to the optical, the UV brightness decays first steeply and then shallower due to radioactive decay of Nickel and Cobalt. The uvm2 photometry is much fainter than the other bands, so the points have larger errors, but the light curves seem to be broader (decaying shallower) than the other UV filters. In Table 2 we report the typical decay rate in mags/100 days as in Pskovskii (1967), with  $\beta$  representing the early decay and  $\gamma$  the later shallow decay. The UV lightcurves of SNe Ia are fairly uniform, and the uvw1 curves match well with the HST/IUE spectrophotometry of SN 1992A in the comparable F275W band (Kirshner et al. 1993; Brown et al. 2005; Milne et al. 2007). More details on the lightcurves and generation of UV lightcurve templates for SNe Ia will be presented in Milne et al. (in preparation).

From a sample of light curves one can begin to discern what is normal and what is peculiar behavior. Two SNe Ia that stand out are SNe 2005hk and 2005ke. SN 2005hk was already fading in the UV when *Swift* observations began, nearly 10 days before the optical maximum. SN 2005ke followed the typical Ia decay until about 15 days after maximum light when the UV brightness remained nearly constant for  $\sim 20$  days before fading again. In conjunction with a marginal x-ray detection, this plateau in the UV light curves has been attributed to interaction with the circumstellar material (Immler et al. 2006), though other causes such as reduced line blanketing have been suggested (Kasliwal et al. 2008). Contamination could be ruled out for SN 2005ke because the first observation showed the SN fainter than the plateau level and subsequent observations showed it had faded again. For other SNe contamination is harder to rule out, but SNe 2007ax (Kasliwal et al. 2008) and 2006mr show hints of extended emission above the background. SN 2006E also stands out with its relatively flat light curves, but that is because the peak and early decay were missed and the slow decay merely represents the shallower late time decay also seen in other SNe Ia.

For SNe Ib/c, the sample of well observed SNe is much smaller, with 3 light curves in our sample, but they appear to be as diverse in the UV as they are in the optical (see Fig. 3). Other SNe Ib/c were also observed but for only a single epoch or were not well detected (see Holland et al. (2007) for additional SNe Ib/c observed during *Swift's* first two years). It is hard to define a generic UV behavior, so instead we briefly describe each well sampled SN.

SN 2006aj, a Ic SN, was discovered following *Swift* BAT trigger on GRB060218 (Campana et al.

2006). The UV initially rose rapidly reaching a bright peak about half a day after the trigger. This first peak has been attributed to the shock breakout from a dense stellar wind (Campana et al. 2006; Blustin 2007; Waxman, Meszaros, & Campana 2007) or self-absorbed synchrotron radiation (Ghisellini, Ghirlanda, & Tavecchio 2007). This faded rapidly in the UV, plateauing briefly from 4–10 days after the trigger as the radioactive decay powered a supernova light curve, and then faded again. In uvw2 and uvm2 this SN peaked 4 magnitudes fainter than the earlier peak. The optical curves are consistent with a SN Ic of intermediate luminosity between normal SNe Ic and previous GRB-associated, overluminous SNe Ic (cf. Pian et al. 2006 and Modjaz et al. 2006).

SN 2006jc was a peculiarly bright and blue SN Ib (Foley et al. 2007), and the UVOT grism spectra show an indication of MgII emission (Immler et al. 2008). Discovered near maximum light, the UV and optical light curves all fade steeply and then shallower and then steeper again. The UVOT light curves will be studied in more detail in Modjaz et al. (in preparation). SN 2007Y, a peculiar Ib/c with spectral similarities to SN 2005bf (Folatelli et al. 2007), behaved more like a Ia in shape and color with the UV brightness rising with the optical, peaking a little sooner and fading slightly quicker.

SNe IIP start off very bright and blue. Brightening to a maximum just a few days after explosion, the UV magnitudes then fade rather linearly, with the uvm2 filter decaying slightly faster than the others. Individual light curves of the SNe IIP are displayed in Fig. 3. This rapid drop in the UV brightness is driven by the cooling photosphere and the resulting line blanketing of heavy elements (cf. Brown et al. 2007a). Dessart et al. (2007) compare the UVOT photometry of SNe II 2005cs and 2006bp with model spectra and demonstrate the usefulness of UV photometry in constraining the extinction and the temporal change in temperature and ionization. The optical brightness remains constant, resulting in a steady reddening with time. While this reddening is common to all the SNe IIP observed by UVOT, the decay slopes vary by nearly a factor of 2 (as shown in Table 2), possibly reflecting the different cooling rates of the SN photospheres.

In order to better contrast the SN types, Fig. 4 shows the UVOT light curves of a well observed example of each type. For easy comparison, the time and magnitude axis are the same across the plots and the magnitudes are unshifted to show the relative colors. The explosion dates for SNe 2007af and 2007Y assume a rise time of 18 days to the maximum light in the V band for SNe Ia/b/c (Garg et al. 2007; Stritzinger et al. 2002), while SN 2006bp uses the explosion date determined by Dessart et al. (2007). The main SN subtypes missing from our sample are SNe IIL, IIn, and Iib. Fortunately, examples of these classes, along with the peculiar SN II 1987A were well observed with IUE and HST, making these sets complementary.

#### 4. COLORS

In addition to physical properties like temperature and extinction, UV and UV-optical colors are also useful in differentiating SN types. The use of optical colors to distinguish SNe of different types has

TABLE 2  
DECAY SLOPES

Filter	SN Ia $\beta$ (mag/100 d)	SN Ia $\gamma$ (mag/100 d)	SN Ibc $\beta$ (mag/100 d)	SN II $\beta$ (mag/100 d)
uvw2	9--10	3	18	23--37
uvm2	7--9	3	14	23--41
uvw1	11--13	2	18	20--32

NOTE. — SNe used: Ia  $\beta$  (SNe 2007af, 2005ke), SN Ia  $\gamma$  (SN 2006E), SN Ibc  $\beta$  (SN 2007Y), SN II  $\beta$  (SNe 2005cs, 2006at, 2006bp)

been explored by multiple authors (Vanden Berk et al. 2001; Poznanski et al. 2002; Gal-Yam et al. 2004; Sullivan et al. 2006; Kuznetsova & Connolly 2007; Poznanski & Maoz 2007). These techniques are of primary importance for large and deep surveys and searches for which the SN candidates are either too faint or too numerous for spectroscopic classification of all candidates. The upcoming Pan-STARRS could discover on the order of 10,000 SNe/year<sup>12</sup> and the Large Synoptic Survey Telescope 250,000 SNe/year.<sup>13</sup> Thus photometric measures of the SNe will be critical to classifying SNe, as well as determining photometric redshifts. Rest frame UV observations can greatly improve the accuracy of such determinations. Fig. 6 compares the color-color location of two SNe Ia (SNe 2007af and 2005ke, well observed examples of a normal and sub-luminous Ia respectively) and two SNe IIP (the well observed SNe 2005cs and 2006bp) in the 5 colors (using neighboring filter combinations) available from the UVOT observations. Extinction vectors, corresponding to a color excess  $E(B-V)=0.1$  and the Milky Way extinction law (Cardelli, Clayton, & Mathis 1989) evaluated at the central wavelengths, are plotted in each color-color plot, though the effect of extinction can vary with different source spectra and choices of extinction laws. As the UVOT  $u$ ,  $b$ , and  $v$  magnitudes are similar to the Johnson  $UBV$ , the bottom right panel is comparable to Fig. 3 in Poznanski et al. (2002). In those colors there is still a lot of overlap between SNe Ia and II. As one adds progressively bluer filters, SNe Ia and II are better separated, showing the advantage of rest-frame UV observations. In the upper left panel, SNe Ia are actually bluer than SNe II in the uvw2-uvm2 color, but this is likely due to the red tail of the uvw2 filter allowing more optical photons through and making the uvm2 look fainter by comparison. As discussed more below, the UV and UV-optical colors of SNe II evolve dramatically, making their colors more similar to SNe Ia.

This clear difference between the UV-bright SNe II and the UV-faint SNe Ia was noticed after a few IUE observations of SNe Ia and II (Panagia 1982, see also Panagia 2003). This "UV deficit" is caused by the very red Ia spectrum between  $\sim 2500$  and  $4000 \text{ \AA}$  (cf. Kirshner et al. 1993), and was exploited by Riess et al. (2004) to identify SNe Ia in the Hubble Deep Field. The left panel of Fig. 6 uses filters on either side and in the middle of that red spectral slope to give two colors, uvm2-uvw1 and uvw1-b, which best show the contrast between SNe Ia and II.

<sup>12</sup> <http://pan-starrs.ifa.hawaii.edu/project/reviews/PreCoDR/documents/scienceproposals/sne.pdf>

<sup>13</sup> [http://www.lsst.org/Science/fs\\_transient.shtml](http://www.lsst.org/Science/fs_transient.shtml)

The SNe II are clearly separated into the top left portion of the plot, while the SNe Ia are in the bottom right. The  $uvw1-b$  color is sufficient by itself to make the distinction, with  $uvw1-b \lesssim 1$  corresponding to young SNe II. The right panel of Fig. 6 adds the colors of our three SNe Ib/c, spanning the range of colors seen in SNe Ia and II, complicating their differentiation. The similarities of SN 2006jc with SNe IIn (Pastorello et al. 2008) explains the blue UV-optical colors. More typical SNe Ib/c have lower effective temperatures and the subsequent UV line blanketing make their colors more similar to SNe Ia. The contamination of SNe Ib/c from cosmological samples of SNe Ia, as discussed in Riess et al. (2004), is reduced because the SNe Ib/c are less common and usually much fainter than SNe Ia.

While red UV-optical colors differentiate well between young SNe II and Ia, they are not conclusive, as SNe II become redder with time. In Fig. 7 we display the  $uvw1-b$  color evolution of these same SNe. To determine the explosion date we have assumed a rise time of 18 days to the maximum light in the V band for SNe Ia (Garg et al. 2007) and for the SNe II we use the explosion times determined by Dessart et al. (2007). At early times, there is a 3 magnitude difference between the  $uvw1-B$  color of SNe Ia and II. However, this large difference does not persist as the SN II temperature (and correspondingly the UV flux) drops with time creating a redder spectrum whose colors become similar to SNe Ia (whose red colors evolve rather slowly) by day 20. Fransson et al. (1987) noticed this rapid reddening in SN 1987A and cautioned against using the UV alone to distinguish SNe I from II. Even a rough determination of the SN epoch, through either the light curve behavior or even the cadence of the SN search observations can help make the distinction. Reddening is a further degeneracy which can also be broken by monitoring the color evolution, as reddening would cause a shift in the colors at a given epoch but not mask the differing slopes of the color evolution.

Understanding the UV color differences within and across types is especially important for classifying high redshift SNe. Some UV information is being incorporated into such phototyping (cf. Riess et al. 2004; Johnson & Crots 2006) but in the past has been limited due to the limited epochs at which UV information is available. The addition of this UV photometry should help improve the understanding of the diversity and temporal change of the UV flux to allow SNe to be better identified at larger redshifts. Other high redshift applications are discussed below.

### 5. HIGH REDSHIFT APPLICATION

In addition to SN observations by UV satellites, deep optical observations will observe the rest-frame UV light from higher redshift SNe. Fig. 8 displays the rest frame UV light sampled by the UVOT UV filters as it corresponds to observed wavelengths as a function of redshift, highlighting regions where the UV filters correspond well with commonly used optical and infrared filters. To highlight the regions where the overlap between the filters is greatest, the bands are centered on the central wavelength and extend one quarter of the full width half max of the filter transmission in both directions (Poole et al. 2008; Fukugita et al. 1996; Hewett et al. 2006). This graphically depicts useful regions of overlap. For ex-

ample, the photons corresponding with the rest-frame  $uvw1$  begins to be redshifted into the optical  $u'$  band (e.g. SDSS-II SN survey; Sako et al. 2008; and LSST) for objects at a redshift of  $z \sim 0.4$  and the  $g'$  band (e.g. SNLS; Astier et al. 2006) at  $z \sim 0.8$ , where the  $u'-g'$  colors also correspond well with our  $uvw2-uvw1$  colors. While chasing the optical light to high redshifts will require observing into the infrared, the use of rest frame UV light can be done with optical and near-IR observations possible with current and planned large ground based telescopes.

Aldering et al. (2006) discuss many uses for rest-frame UV observations of these high redshift SNe in the context of SNAP, and this local sample should allow a comparison looking for evolutionary effects. Since SNAP is planned to have logarithmically spaced filters beginning at 4000 Å, they will cover the restframe UV observed by the UVOT filters for redshifts beyond  $z \sim 0.8$ . More generally, any deep SN search optimized for finding and following high redshift SNe in the optical will likely also detect the rest-frame UV light of SNe (preferentially SNe II due to their brighter UV luminosities) at the high end of their target redshift and beyond. Measuring SN rates at higher redshifts is only one of many uses of these high redshift detections. Making full use of this data will require a better understanding of the UV light best obtained for nearby SNe for which multi-wavelength photometry and spectroscopy over a larger portion of the light curve is possible. Rest-frame UV observations of a local sample of SNe have the further advantage of being a comparison sample with which to understand the high redshift SNe, look for evolutionary differences (see e.g. Foley et al. 2007; Ellis et al. 2008), and further constrain photometric redshifts, extinction, and luminosity distances.

### 6. FUTURE WORK

We have presented here the largest collection of UV light curves obtained by any single instrument, which have allowed the study of individual objects as well as comparisons within and across SN types. In addition to these apparent magnitudes, we are also working to calibrate the absolute magnitudes to many of these objects (Brown et al. in preparation). The absolute magnitudes can be used to study the utility of rest frame UV observations for cosmological measurements and for determining high redshift SN rates. We are also combining this data with optical and near-infrared observations to construct bolometric lightcurves that encompass more of the spectrum for individual objects and refining bolometric corrections used in constructing bolometric curves from optical data alone (cf. Contardo, Leibundgut, & Vacca 2000). The light curve shapes and colors of our large sample should also help in the classification of SNe, particularly at higher redshifts when spectra are unobtainable and fewer rest-frame optical bands are observable. Future UV observatories, including a refurbished HST, TAUVE (Safonova, Sivaram, & Murthy 2007), WSO-UV (Pagano et al. 2008) and others, as well as optical observatories observing the high redshift universe, can also benefit from these light curves to better understand and plan effective UV SN observations.

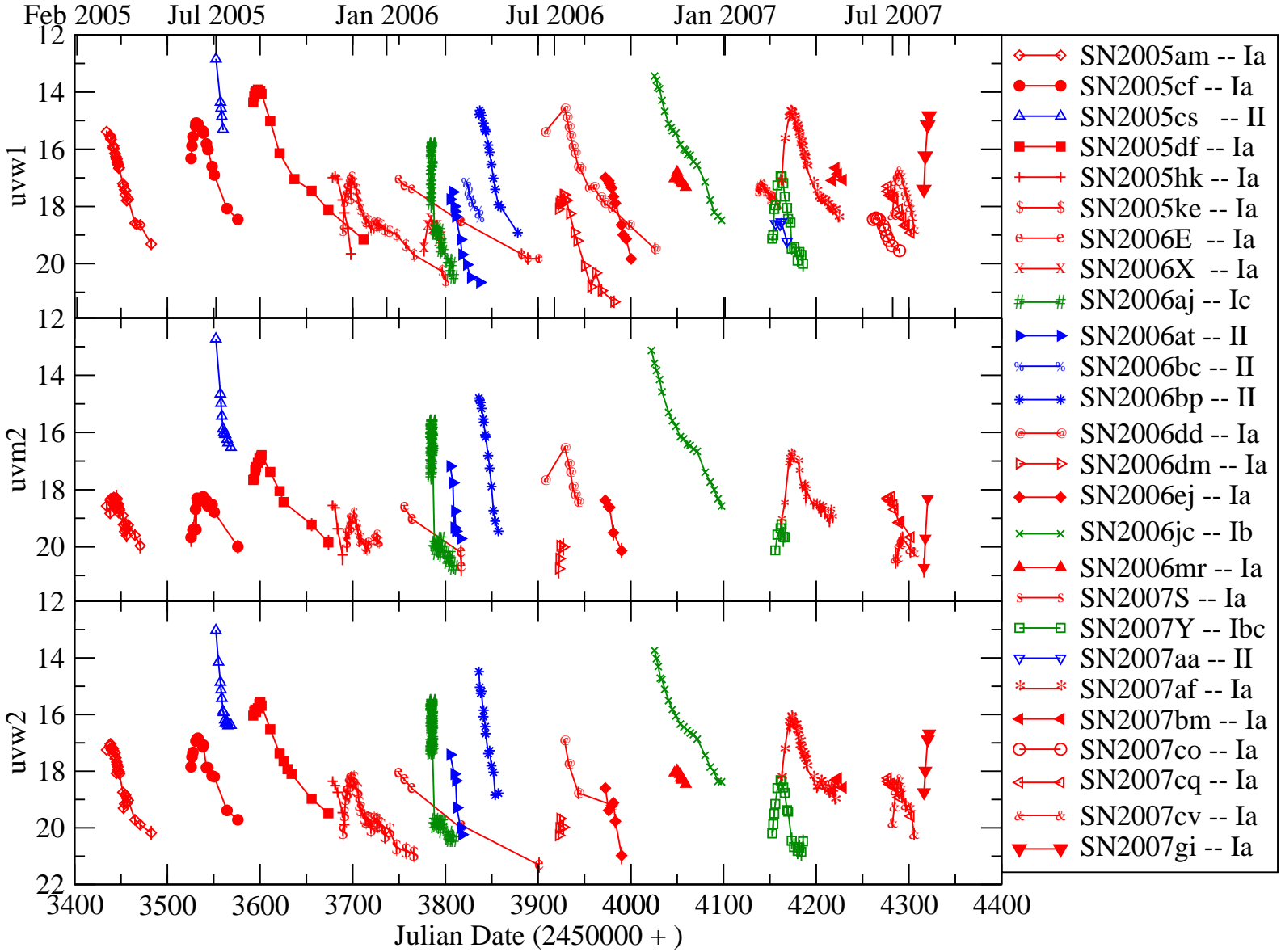
This work made use of public data from the *Swift* data archive. This work is supported at Penn State by NASA

Contract NAS5-00136 and *Swift* Guest Investigator grant NNH06ZDA001N.

#### REFERENCES

- Aldering, G., Kim, A. G., Kowalski, M., Linder, E. V., & Perlmutter, S. 2007, *Astroparticle Physics*, 27, 213
- Astier, P. et al. 2006, *A&A*, 447, 31
- Blustin, A. J., 2007, *Phil. Trans. Roy. Soc.*, p. 1263
- Brown, P. J., et al. 2005, *ApJ*, 635, 1192
- Brown, P. J., et al. 2007, *ApJ*, 659, 1488
- Brown, P. J., Roming, P. W. A., Vanden Berk, D. E., Holland, S. T., Immler, S., & Milne, P. A., 2007, in *AIP Conf. Proc.* 937, *SUPERNOVA 1987A: 20 YEARS AFTER: Supernovae and Gamma-Ray Bursters*, ed. S. Immler & K. Weiler, 386-390 (arXiv:0802.3465)
- Campana et al., 2006, *Nature*, 442, 1008
- Cappellaro, E., Turatto, M., & Fernley, J. 1995, in *IUE-ULDA Access Guide #6 – Supernovae*, ESA
- Cardelli, Clayton, & Mathis, 1989, *ApJ*, 345, 245
- Contardo, G., Leibundgut, B., & Vacca, W.D., 2000, *A&A*, 359, 876
- Dessart, L., et al. 2008, *ApJ*, 675, 644
- Ellis, R. S., et al., 2008, *ApJ*, 674, 51
- Foley, R. J., et al. 2007, *ApJ*, submitted (astro-ph/0710.2338)
- Folatelli, G., Morrell, N., Phillips, M., & Hamuy, M. 2007, *CBET* 862
- Fransson, C., Grewing, M., Cassatella, A., Panagia, N., & Wamsteker, W. *A&AL*, 177, 33
- Fukugita, M., Ichikawa, T., Gunn, J. E., Doi, M., Shimasaku, K., & Schneider, D. P. 1996, *AJ*, 111, 1748
- Gal-Yam, A., Poznanski, D., Maoz, D., Filippenko, A. V., & Foley, R. J. 2004, *PASP*, 116, 597
- Garg, A., et al., 2007, *AJ*, 133, 403
- Gehrels, N., et al. 2004, *ApJ*, 611, 1005
- Ghisellini, G., Ghirlanda, G., & Tavecchio, F. 2007, *MNRASL*, 37
- Hewett, P. C., Warren, S. J., Leggett, S. K., & Hodgkin, S. T. 2006, *MNRAS*, 367, 454
- Holland, S. T., Immler, S., Brown, P. J., Roming, P. W. A., Vanden Berk, D., & Milne, P. A., 2007, in *AIP Conf. Proc.* 937, *SUPERNOVA 1987A: 20 YEARS AFTER: Supernovae and Gamma-Ray Bursters*, ed. S. Immler & K. Weiler, 391
- Holm, A. V., Wu, C., & Caldwell, J. J., 1974, *PASP*, 86, 296
- Immler, S. et al. 2005, *ApJ*, 632, 283
- Immler, S. et al. 2006, *ApJ*, 648, L119
- Immler, S. et al. 2008, *ApJL*, 674, 85
- Jeffery, D. J., et al., 1994, *AJ*, 421, L27
- Johnson, B. D. & Crotts, A. P. A., 2006, *AJ*, 132, 756
- Kasliwal, M. 2008, *ApJL*, submitted
- Kirshner, R. P., et al. 1993, *ApJ*, 415, 589
- Kuznetsova, N. V., & Connolly, B. M. 2007, *ApJ*, 659,530
- Lentz, E. J., Baron, E., Branch, D., Haushildt, P. H., & Nugent, P. E. 2000, *ApJ*, 530, 966
- Li, W., Jha, S., Filippenko, A. V., Bloom, J. S., Pooley, D., Foley, R. J., & Perley, D. A. 2006, *PASP*, 118, 37
- Lyubimkov, L. S., 1990, *Soviet Astron.*, 34, 239
- Milne, P. A., Brown, P. J., Holland, S. T., Roming, P. W. A., & Immler, S., 2007, in *AIP Conf. Proc.* 937, *SUPERNOVA 1987A: 20 YEARS AFTER: Supernovae and Gamma-Ray Bursters*, ed. S. Immler & K. Weiler, 303
- Modjaz, M., et al. 2006, *ApJL*, 645, 21
- Nugent, P., et al., 1997, *ApJ*, 485, 812
- Pagano, I., et al., 2008, arXiv:0801.2039
- Panagia, N. 1982, some IUE conf. proc.
- Panagia, N., 1985, in *Harvard CFA Workshop “Supernovae as Distance Indicators”*, ed. N. Bartel, Springer-Verlag, p.14-33
- Panagia, N. 2003, in *Supernovae and Gamma-Ray Bursters*. ed. K. Weiler, 598, 113
- Panagia, N. et al. 1980, *MNRAS*, 192, 861
- Pastorello, A., et al. 2008, *MNRAS*, submitted (arXiv:0801.2277)
- Pian, E., et al. 2006, *Nature*, 442, 1011
- Poole, T. et al., 2008, *MNRAS*, 383, 627
- Poznanski, D., et al. 2007, *MNRAS*, 382, 1169
- Poznanski, D., & Maoz, D. 2007, *AJ*, 134, 1285
- Poznanski, D., Gal-Yam, A., Maoz, D., Filippenko, A. V., Leonard, D. C., & Matheson, T. 2002, *PASP*, 114, 833
- Pskovskii, U. P., 1967, *Sov. Astron.*, 11, 63
- Pun, C. S. J. et al. 1995, *ApJSS*, 99, 223
- Riess, A. G. et al. 2004, *ApJ*, 600, L163
- Roming, P. W. A., et al. 2005, *Space Science Reviews*, 120, 95
- Safonova, M., Sivaram, C., & Murthy, J. 2007, arXiv:0712.3354
- Sako, M. et al. 2008, *AJ*, 135, 348
- Stritzinger, M., et al., 2002, *AJ*, 124, 2200
- Sullivan, M., et al., 2006, *AJ*, 131, 960
- Vanden Berk, D. E., et al. 2001, *BAAS*, 199.8405
- Wang, L., Aldering, G., Filippenko, A. V., Challis, P., Nugent, P., Li, W., Matheson, T., & Howell, A. 2005, *BAAS*, 206.4501
- Waxman, E., Meszaros, P., & Campana, S., 2007, *ApJ*, 667, 351

FIG. 1.— UV light curves of SNe well detected in at least three epochs by UVOT. SNe Ia are displayed in red, SNe Ib/c in green, and SNe II in blue.



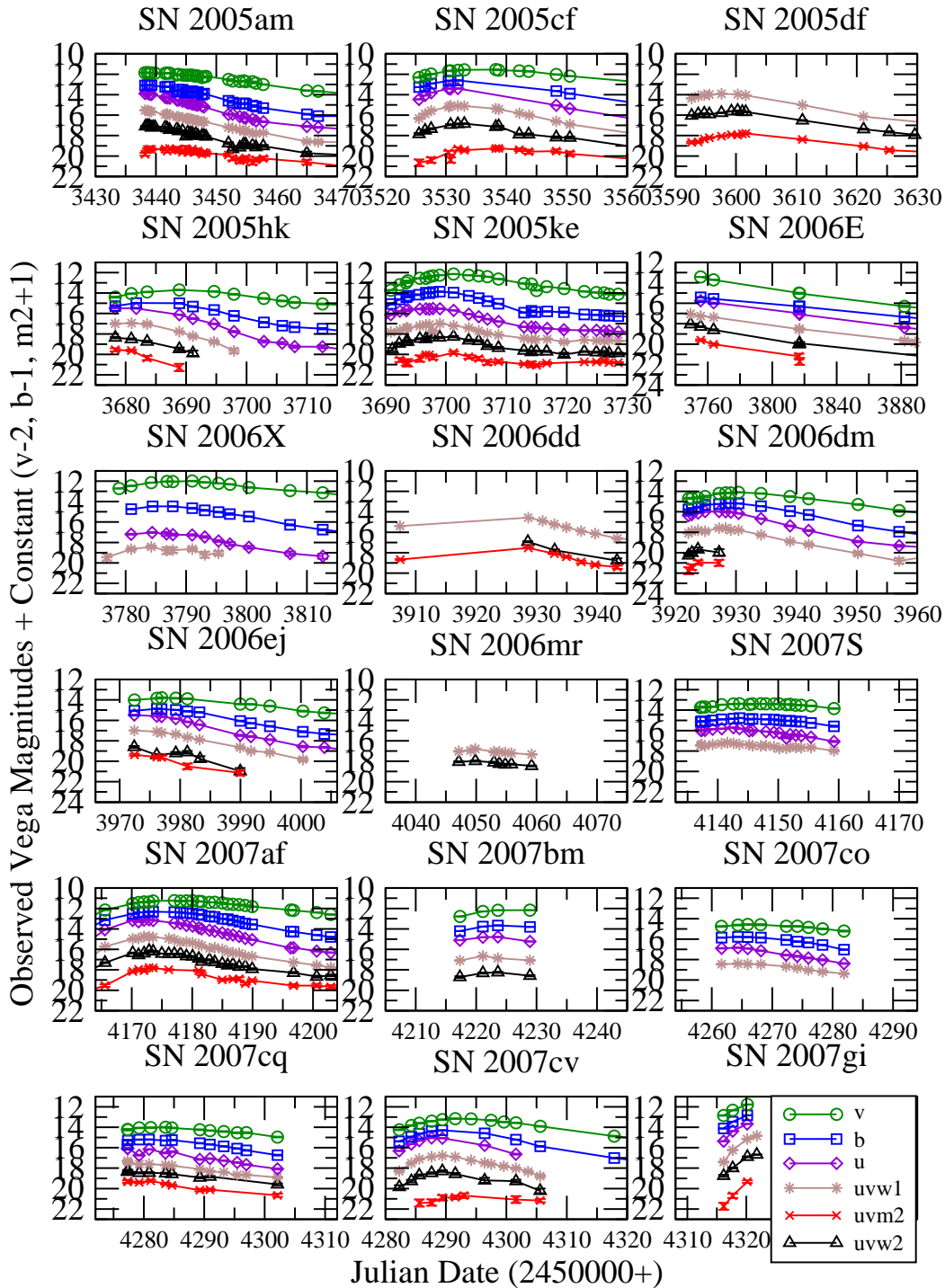


FIG. 2.— UVOT light curves of 18 SNe Ia. The curves have been offset by v-2, b-1, and uvm2+1 for clarity. For comparison purposes the axis are on the same scale, showing the 40 days around maximum light (with the exception of SN2006E which was only observed well after maximum).

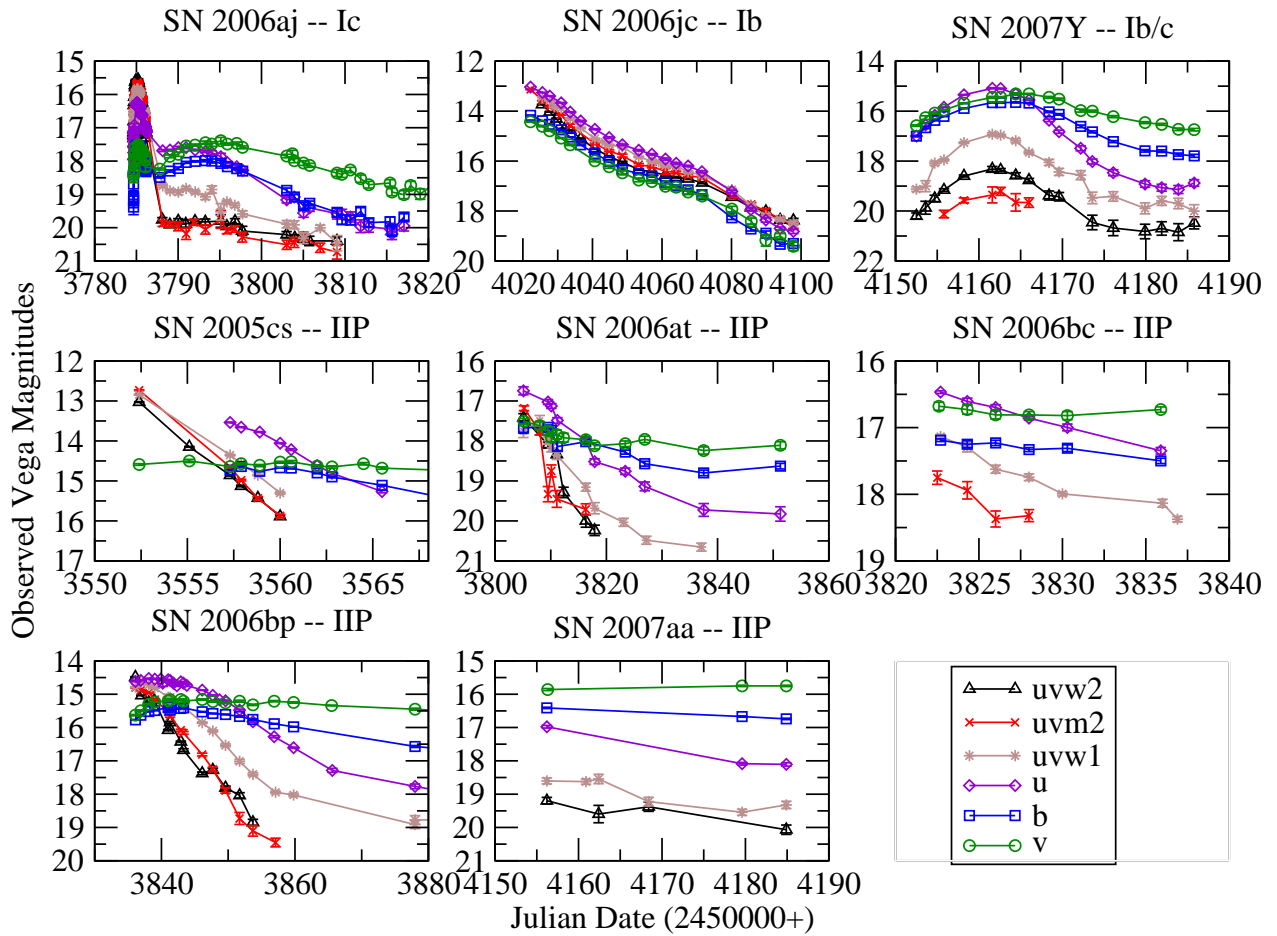


FIG. 3.— UVOT light curves of 3 SNe Ib/c and 5 SNe II.

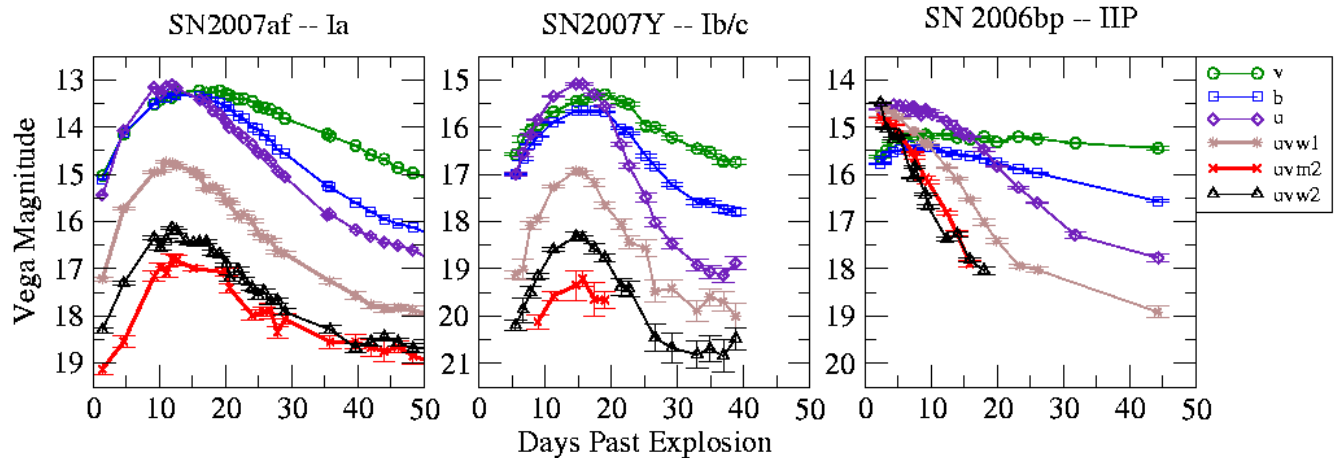


FIG. 4.— UVOT light curves of SN 2007af (Ia), SN 2007Y (Ib/c), and SN 2006bp (IIP). The observed magnitudes have not been shifted and the horizontal and vertical axis are scaled the same to allow relative colors and slopes to be compared by eye.



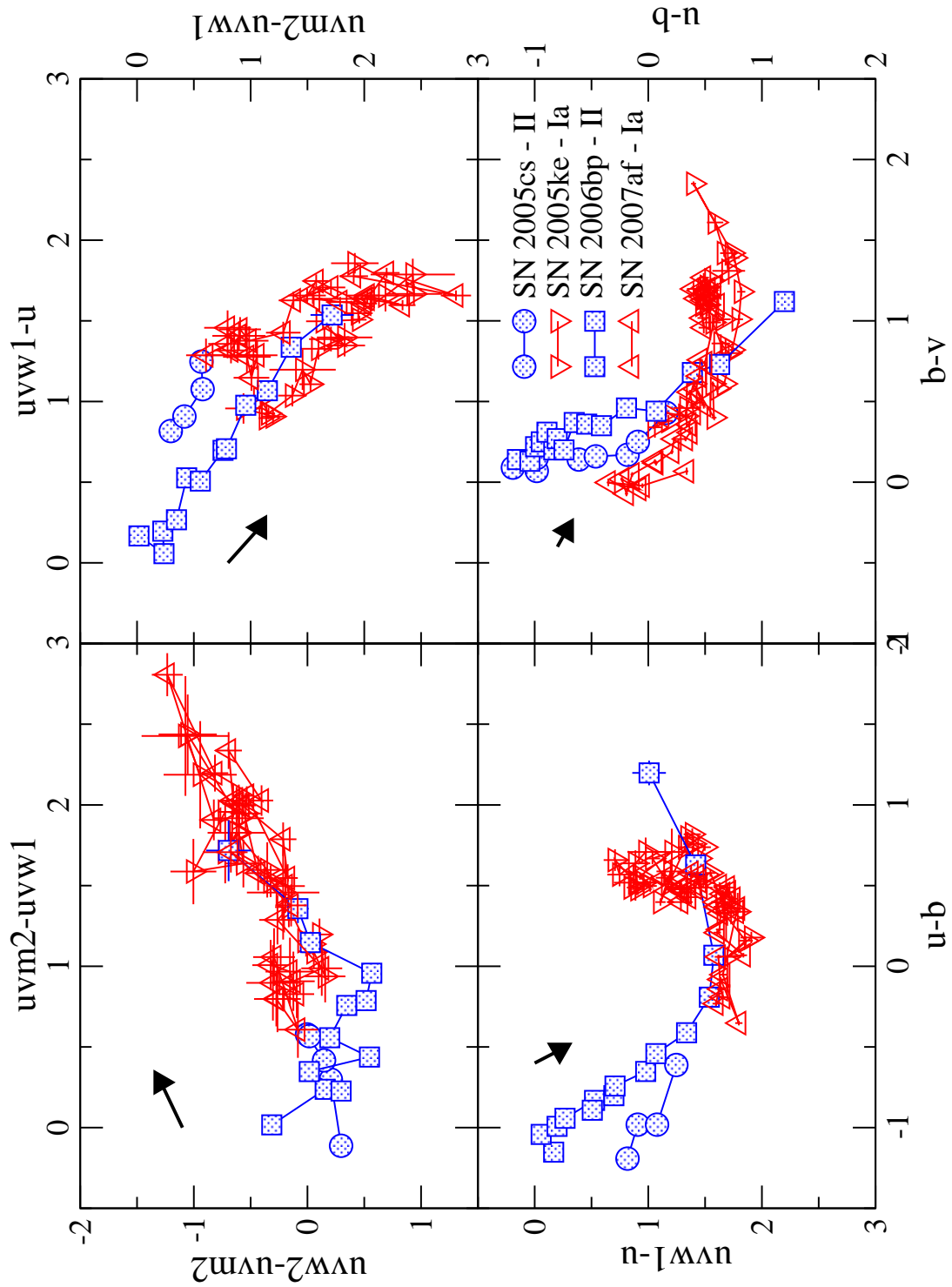


FIG. 5.— Color-color plots showing the differentiation of young SNe II from SNe Ia. The ability to differentiate the two increases at shorter wavelengths due to the contrasting spectral shapes. The arrows are extinction vectors corresponding to  $E(B-V)=0.1$  computed using the MW extinction relations of Cardelli, Clayton, & Mathis (1989) evaluated at the central wavelength of the UVOT filters. Note that MW extinction actually causes bluer  $uvw2-uvw2$  colors due to the  $uvw2$  filter coinciding with the 2200 Å bump in the MW extinction curve rather than the typical “reddening” effect of extinction.

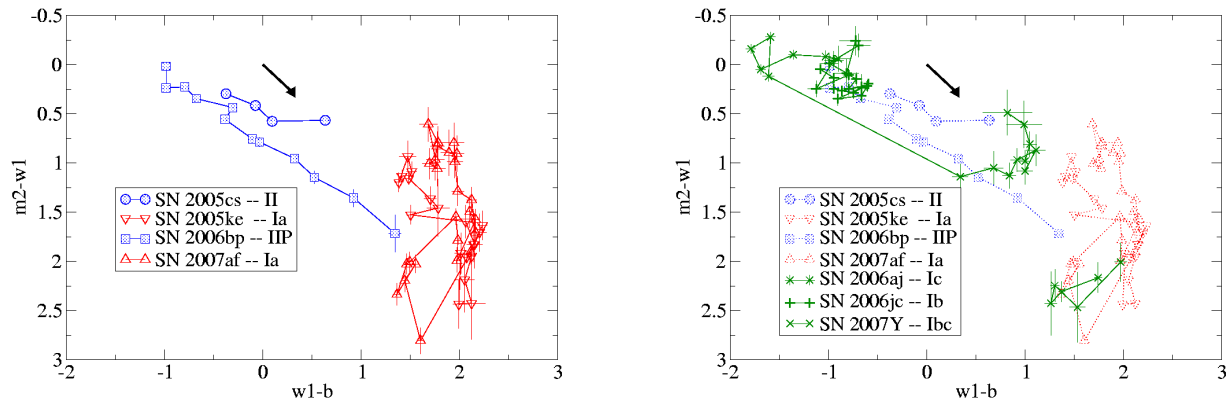


FIG. 6.— Left panel:  $uvw_2 - uvw_1$  v.  $uvw_1 - b$  color color plots showing the clear differentiation of young SNe II from SNe Ia. The SNe Ia are in red, and the SNe IIP in blue. The right panel shows the location of our 3 SNe Ib/c (marked in green) in the same color-color space. The arrows correspond to the  $uvw_1 - b$  color change of MW extinction corresponding to  $E(B-V)=0.1$ .

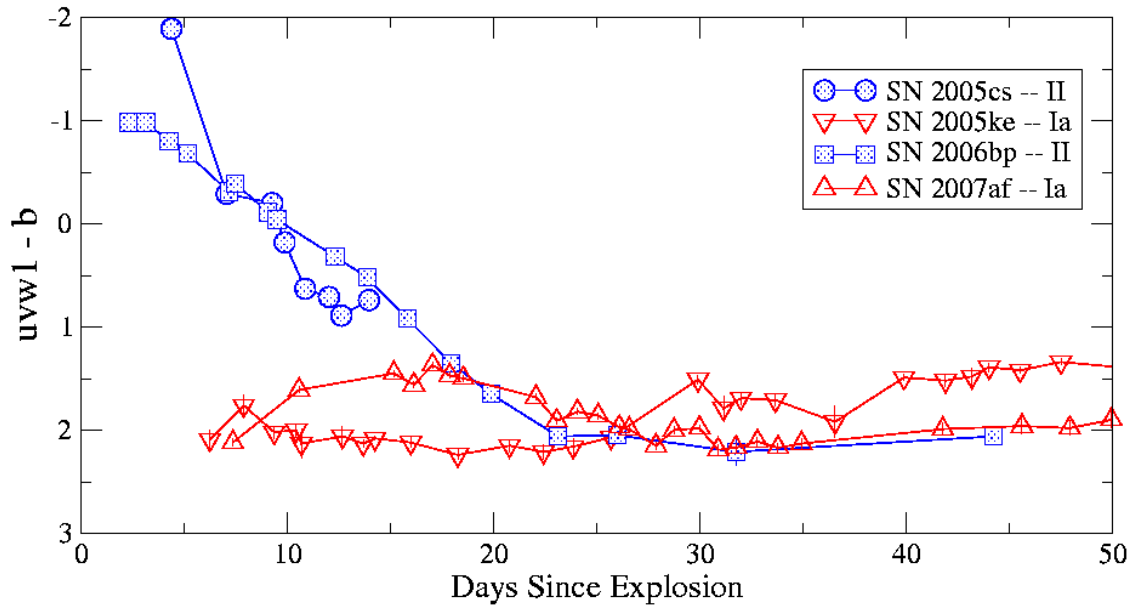


FIG. 7.— UV-optical color evolution of two SNe Ia and two SNe IIP. The symbols are the same as used in the above color-color plots. The dramatic color difference at early times vanishes by about 20 days after the explosion.

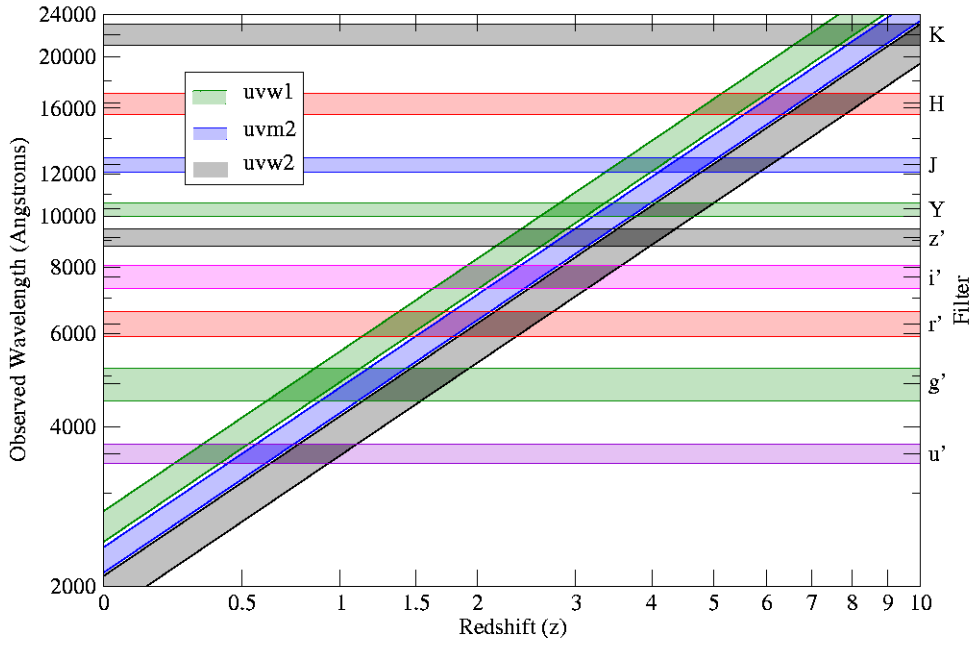


FIG. 8.— Rest frame UV light sampled by the UVOT UV filters as it corresponds to observed wavelengths as a function of redshift. The observed wavelength ranges for commonly used filter sets (optical–SDSS (Fukugita et al. 1996) and infrared–UKIRT set (Hewett et al. 2006)) are also highlighted.